

Biosynthesis of Magnetite (Fe₃O₄) Nanostructures using *Vernonia Amygdalina* Leaves Extract

Asratemedhin B. Habtemariam ¹ 

¹ Physics Department, College of Natural and Computational Sciences, Debre Berhan University, P. O. Box 445, Ethiopia

* Correspondence: asratemedhinbekele@dbu.edu.et (A.B.H);

Scopus Author ID: 57212268225

Received: 6.02.2021; Revised: 5.04.2021; Accepted: 10.04.2021; Published: 9.05.2021

Abstract: An eco-friendly biosynthesis route was employed to synthesize magnetite nanostructures using *Vernonia amygdalina* leaves extract as a reducing and chelating agent and ferric nitrate nonahydrate precursor at ambient conditions. The desired phase formation and crystal structure of the synthesized nanostructures were in cubic face-centered as confirmed by X-ray diffraction analysis. Morphological properties were studied by scanning electron micrograph, and it showed that nanostructures were synthesized. Ultra-violet visible spectrometer was used to study the optical properties, and ultra-violet visible analysis revealed that spectral absorption band occurred at about 396 nm, which is a characteristic feature of iron oxide. From the Fourier-transform infrared spectrometer analyses of functional groups, the appearance of peaks at 561 cm⁻¹ and 461 cm⁻¹ also corroborate the formation of Fe₃O₄ nanostructures.

Keywords: biosynthesis; nanostructures; *Vernonia amygdalina*; magnetite.

© 2021 by the authors. This article is an open-access article distributed under the terms and conditions of the Creative Commons Attribution (CC BY) license (<https://creativecommons.org/licenses/by/4.0/>).

1. Introduction

Iron exists in more than a dozen of oxidation states in nature [1]. The commonly known iron oxides hematite (α -Fe₂O₃), maghemite (γ -Fe₂O₃), and magnetite (Fe₃O₄) are promising candidates for various technological applications due to their polymorphism involving temperature-dependent phase transition [2]. As a result of its hydrophilic and biocompatibility properties, Fe₃O₄ has received enormous attention for various applications such as wastewater treatment, pigment, magnetic resonance imaging, and biomedical applications [3-6]. However, due to its thermodynamic instability, there is a limitation in the technological applications of Fe₃O₄ [7]. Fe₃O₄ possesses an inverse spinel structure with the Fe³⁺ ions distributed randomly between octahedral and tetrahedral sites and the Fe²⁺ ions occupying the octahedral sites [6].

Now a day, several synthetic methods such as co-precipitation [7-9], thermal decomposition [3], hydrothermal [5, 10, 11], sol-gel [12], micro-emulsion [13], sonochemical synthesis [14], microwave combustion [15] and biological synthesis [1, 16] have been employed to produce Fe₃O₄ nanostructures. Among these, nanostructures' biosynthesis is an alternative compared to conventional methods since it is non-toxic, eco-friendly, and can control the size and shape of synthesized nanoparticles [17, 18]. For instance, magnetite iron oxide nanoparticles were successfully synthesized using an aqueous extract of spent tea waste as a reducing agent [19]. Similarly, magnetic iron oxide nanoparticles with an average crystallite size of 18 nm were synthesized from *Sargassum muticum* aqueous extract as a

reducing agent [20]. Nano-sized iron particles were also successfully synthesized using leaf extract of Mint (*Mentha spicata L.*) plant [21]. In the present study, we used *Vernonia amygdalina* (*V. amygdalina*) leaves aqueous extract to successfully synthesize magnetite nanostructures.

V. amygdalina is a small shrub, three-five meters tall, mostly distributed in tropical Africa [22-24]. The plant is commonly called *bitter leaf* due to its bitter taste [23]. *V. amygdalina* ('*Grawa*' in Amharic, Ethiopia) is known for its high production, adaptability, and its ability to improve the soil fertility for better crop production [25]. In the rural highlands of Ethiopia, the water extract of *V. amygdalina* leaves serves as a tonic drink for the prevention of stomach-ache. It exhibits excellent antioxidant property [24], and this has been reported in an attempt to synthesize NiO nanoparticles [26].

2. Materials and Methods

2.1. Materials.

Analytical grade reagents such as ferric nitrate nonahydrate ($\text{Fe}(\text{NO}_3)_3 \cdot 9\text{H}_2\text{O}$, 97% purity) were used in this experiment. Fresh, matured, and healthy *V. amygdalina* leaves were gathered from Debre Birhan town, North Shoa, Ethiopia. Taxonomically authenticated *V. amygdalina* leaves were thoroughly washed with tap water followed by distilled water for removing unwanted impurities such as dust and scum. The leaves were dried at room temperature for a couple of weeks, cut into small pieces, and kept in a tight plastic bag till the experiment.

2.2. Methods.

Weighed 10 gm of the dried leaves were added into 200 mL of deionized water and boiled at 80 °C for about 60 minutes to obtain the aqueous extract (Figure 1a). After cooling down to room temperature, it was filtered using Whatman No.1 filter paper, and the filtrate was stored in a refrigerator at 4 °C for further experiments. On the other hand, 0.1M solution of $\text{Fe}(\text{NO}_3)_3 \cdot 9\text{H}_2\text{O}$ was prepared by dissolving 4 g of $\text{Fe}(\text{NO}_3)_3 \cdot 9\text{H}_2\text{O}$ salts in 100 mL deionized water while stirring for about 15 minutes (Figure 1b).

In a typical experiment, *V. amygdalina* plant leaves extract was added to the 0.1M $\text{Fe}(\text{NO}_3)_3 \cdot 9\text{H}_2\text{O}$ solution in 1:2 ratios by volume until the mixture reaches light black in color.

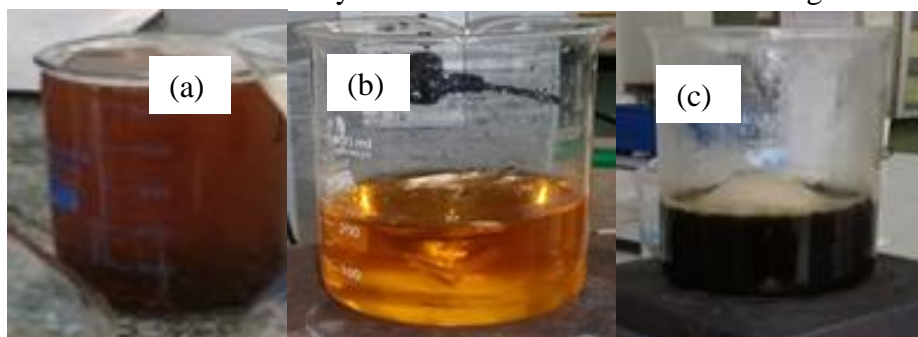


Figure 1. Synthesis procedure of Fe_3O_4 nanostructures. (a) *V. amygdalina* extract; (b) precursor solution; (c) *V. amygdalina* extract + precursor solution.

The resulting mixture was continuously stirred for about 30 min at 50 °C until the solution changes from light black to brownish-black color, revealing the formation of iron

oxide nanostructures (Figure 1c). The solution was then cooled down to room temperature and centrifuged at 3000 rpm for 10 minutes three times, and the precipitates were collected on a Petri dish and oven-dried at 100 °C. Finally, the nanopowder was collected and calcined in an air furnace at 450 °C for 6 hours to get the black iron oxide nanostructures.

3. Results and Discussion

Morphological studies of the biosynthesized Fe₃O₄ nanostructures were confirmed by an X-ray diffractometer (XRD) (Bruker D8 ADVANCED Diffractometer). The XRD patterns of all randomly oriented powder specimen were recorded in the 10° to 80° with 2θ angles using CuKα (λ = 0.15064 nm) whose operating voltage is 40 kV and current of 30 mA with a step size of 0.02°. The XRD peaks for the sample at 18.5°, 30.36°, 35.76°, 43.47°, 53.81°, 57.50°, 63.16°, 66.23°, 71.52°, 74.75°, and 75.77° with the miller indices (111), (220), (311), (400), (422), (511), (440), (531), (442), (620) and (533), respectively, were well matched with JCPDS no. 00-900-5841 and confirmed that the Fe₃O₄ nanostructures were in a face-centered cubic structure. The average crystallite size (D) of Fe₃O₄ is determined from the prominent diffraction peaks at (311) using Scherer's equation to be 5 nm.

$$D = \frac{0.9\lambda}{\beta \cos \theta} \dots\dots\dots(1)$$

where 'D' is the crystallite size, 'k' is the shape factor = 0.9, 'λ' = 0.15406 nm is the x-ray wavelength, 'β' is the full width broadening at half maximum intensity (FWHM) in radians, and 'θ' is the Bragg diffraction angle in radians. Powder XRD patterns of the as-synthesized Fe₃O₄ nanostructures are matched with the standard XRD file of Fe₃O₄, as shown in Figure 2.

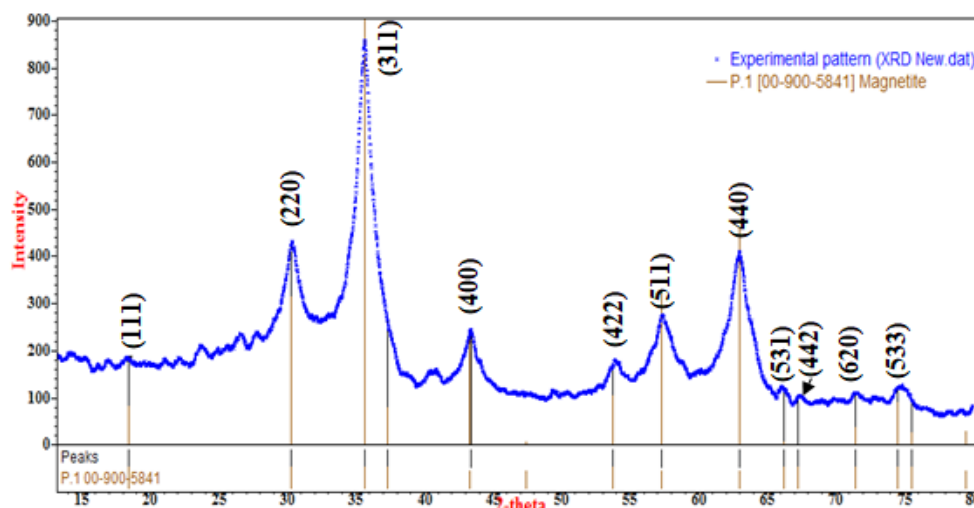


Figure 2. XRD patterns of Fe₃O₄ nanostructures synthesized using *V. amygdalina* leaves extract.

The presence of functional groups responsible for the reduction and stabilization of the Fe₃O₄ nanostructures was confirmed by Fourier transform infrared (FTIR) spectrometer [27]. For FTIR spectral analysis, the as-synthesized powder of Fe₃O₄ was mixed with KBr to prepare pellets that suit the Perkin Elmer 65 instrument, and values were recorded in the wavenumber range of 400–4000 cm⁻¹. Figure 3a shows the FTIR spectrum of *V. amygdalina* plant leaves extract, and the broad absorption band from 3626 cm⁻¹–3175 cm⁻¹ is related to the O–H bond stretching of the phenolic group; the peak at 2082 cm⁻¹ is related to the C–H bending, and the

peak 1638 cm^{-1} is related to the N–H bending [2, 28]. Figure 3b shows the FTIR spectrum of the as-synthesized iron oxide nanopowder. The broadband at 3394 cm^{-1} and 1627 cm^{-1} corresponds to the –OH stretching and bending vibration of water molecules, respectively [7, 15]. The peak at 2916 cm^{-1} corresponds to C–H stretching vibration, and the band at 1394 cm^{-1} indicates C–O bending vibration mode [15]. The peaks at about 561 cm^{-1} and 461 cm^{-1} are due to the Fe–O bond and confirm the formation of spinel-type Fe_3O_4 [7, 15].

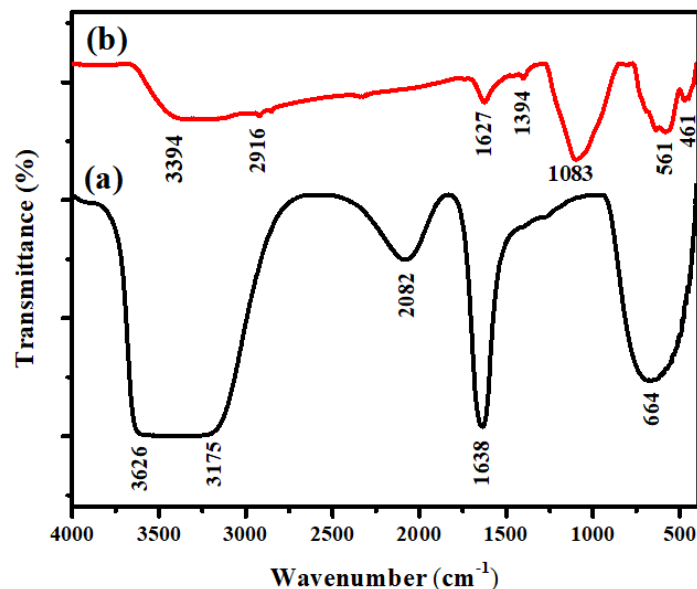


Figure 3. FTIR spectrum of (a) *V. amygdalina* leaves extract; (b) synthesized Fe_3O_4 nanostructures.

The synthesized nanostructures were characterized using a UV–Visible (UV–Vis) spectrophotometer working at a wavelength range of 200–900 nm to study the optical properties.

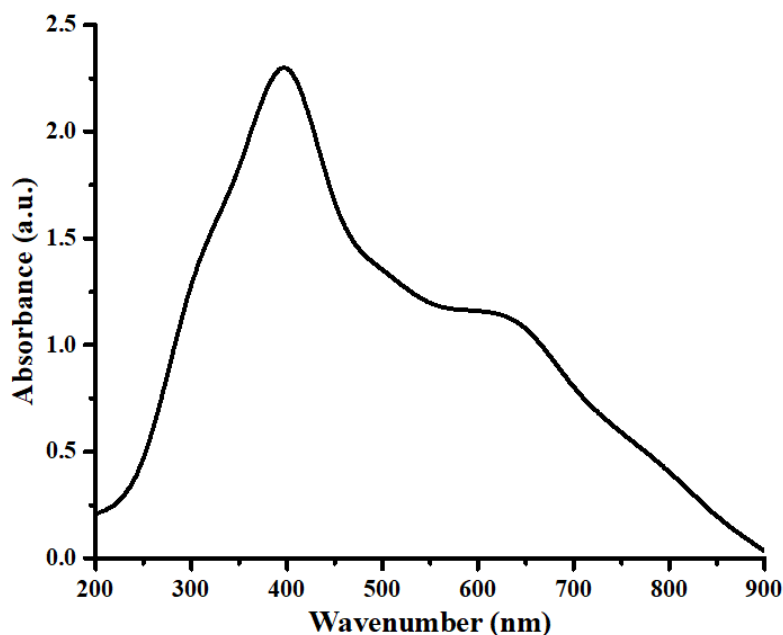


Figure 4. UV–Vis absorption spectra of Fe_3O_4 nanostructures.

The absorption in the visible range of the electromagnetic spectrum affects the perceived color of the chemicals involved. The UV–Visible spectrum of Fe_3O_4 nanostructures synthesized by the extract of *V. amygdalina* leaves is shown in Figure 4. The UV–Vis

spectroscopic study shows the plasmonic resonance property resulting from electronic transitions of molecules and confirmed the reduction of metal ions and formation of Fe₃O₄ nanostructures with a sharp peak at 396 nm [20].

Scanning electron micrograph (SEM) image of the synthesized Fe₃O₄ nanostructures was recorded using JSM–IT 300 LV. The morphology of the as-synthesized Fe₃O₄ using *V. amygdalina* plant extract looks like flakes, as shown in Figure 5. Although XRD analysis shows a face-centered cubic structure, SEM observation does not confirm the cubic structure, which implies that optimization of the work is significant.

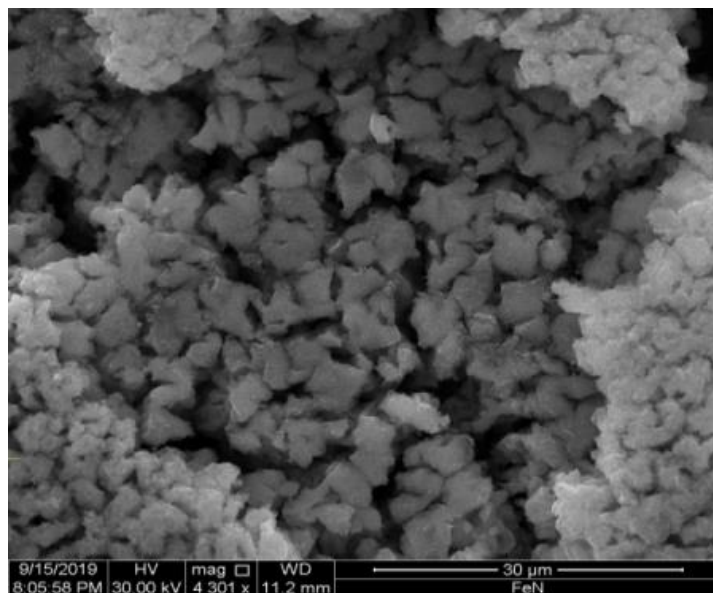


Figure 5. SEM images of Fe₃O₄ nanostructures.

4. Conclusions

Fe₃O₄ nanostructures were successfully synthesized using leaves extract of *V. amygdalina* as reducing and chelating agents at ambient temperature and pressure conditions. Powder XRD patterns revealed the formation of a cubic-face-centered spinel structure. FTIR peaks at 561 cm⁻¹ and 461 cm⁻¹ also support the formation of Fe₃O₄ nanostructures. The UV–Vis spectral absorption band at 396 nm is characteristic of the iron oxide, further affirming Fe₃O₄ nanostructures' formation. SEM image analysis showed that magnetite (Fe₃O₄) nanostructures were successfully synthesized.

Funding

This research received no external funding.

Acknowledgments

The researcher would like to express his heartfelt gratitude to the Materials Science and Engineering Department at Addis Ababa Science and Technology University; Chemistry Department at Addis Ababa University; and Materials Science and Engineering Department at Adama Science and Technology University for running SEM, FTIR, and XRD characterizations, respectively.

Conflicts of Interest

The author declares no conflict of interest.

References

1. Karpagavinayagam, P.; Vedhi, C. Green synthesis of iron oxide nanoparticles using *Avicennia marina* flower extract. *Vacuum* **2019**, *160*, 286-292, <https://doi.org/10.1016/j.vacuum.2018.11.043>.
2. Aisida, S.O.; Madubuonu, N.; Alnasir, M.H.; Ahmad, I.; Botha, S.; Maaza, M.; Ezema, F.I. Biogenic synthesis of iron oxide nanorods using *Moringa oleifera* leaf extract for antibacterial applications. *Applied Nanoscience* **2020**, *10*, 305-315, <https://doi.org/10.1007/s13204-019-01099-x>.
3. Glasgow, W.; Fellows, B.; Qi, B.; Darroudi, T.; Kitchens, C.; Ye, L.; Crawford, T.M.; Mefford, O.T. Continuous synthesis of iron oxide (Fe₃O₄) nanoparticles via thermal decomposition. *Particuology* **2016**, *26*, 47-53, <https://doi.org/10.1016/j.partic.2015.09.011>.
4. Asuha, S.; Suyala, B.; Siqintana, X.; Zhao, S. Direct synthesis of Fe₃O₄ nanopowder by thermal decomposition of Fe-urea complex and its properties. *J. Alloys Compd.* **2011**, *509*, 2870-2873, <https://doi.org/10.1016/j.jallcom.2010.11.145>.
5. Ni, S.; Wang, X.; Zhou, G.; Yang, F.; Wang, J.; Wang, Q.; He, D. Hydrothermal synthesis of Fe₃O₄ nanoparticles and its application in lithium ion battery. *Mater. Lett.* **2009**, *63*, 2701-2703.
6. Klotz, S.; Steinle-Neumann, G.; Strässle, T.; Philippe, J.; Hansen, T.; Wenzel, M.J. Magnetism and the Verwey transition in Fe₃O₄ under pressure. *Physical Review B* **2008**, *77*, 012411, <https://doi.org/10.1103/PhysRevB.77.012411>.
7. Jafari, A.; Shayesteh, S.F.; Salouti, M.; Boustani, K. Dependence of structural phase transition and lattice strain of Fe₃O₄ nanoparticles on calcination temperature. *Indian Journal of Physics* **2015**, *89*, 551-560.
8. Yazdani, F.; Seddigh, M. Magnetite nanoparticles synthesized by co-precipitation method: The effects of various iron anions on specifications. *Mater. Chem. Phys.* **2016**, *184*, 318-323, <https://doi.org/10.1016/j.matchemphys.2016.09.058>.
9. Arévalo, P.; Isasi, J.; Caballero, A.C.; Marco, J.F.; Martín-Hernández, F. Magnetic and structural studies of Fe₃O₄ nanoparticles synthesized via coprecipitation and dispersed in different surfactants. *Ceram. Int.* **2017**, *43*, 10333-10340.
10. Zhu, L.; Zeng, X.; Li, X.; Yang, B.; Yu, R. Hydrothermal synthesis of magnetic Fe₃O₄/graphene composites with good electromagnetic microwave absorbing performances. *J. Magn. Magn. Mater.* **2017**, *426*, 114-120, <https://doi.org/10.1016/j.jmmm.2016.11.063>.
11. Fatima, H.; Lee, D.-W.; Yun, H.J.; Kim, K.-S. Shape-controlled synthesis of magnetic Fe₃O₄ nanoparticles with different iron precursors and capping agents. *RSC Advances* **2018**, *8*, 22917-22923, <https://doi.org/10.1039/C8RA02909A>.
12. Lemine, O.M.; Omri, K.; Zhang, B.; El Mir, L.; Sajjeddine, M.; Alyamani, A.; Bououdina, M. Sol-gel synthesis of 8nm magnetite (Fe₃O₄) nanoparticles and their magnetic properties. *Superlattices Microstruct.* **2012**, *52*, 793-799, <https://doi.org/10.1016/j.spmi.2012.07.009>.
13. Lu, T.; Wang, J.; Yin, J.; Wang, A.; Wang, X.; Zhang, T. Surfactant effects on the microstructures of Fe₃O₄ nanoparticles synthesized by microemulsion method. *Colloids Surf. Physicochem. Eng. Aspects* **2013**, *436*, 675-683, <https://doi.org/10.1016/j.colsurfa.2013.08.004>.
14. Marchegiani, G.; Imperatori, P.; Mari, A.; Pilloni, L.; Chiolerio, A.; Allia, P.; Tiberto, P.; Suber, L. Sonochemical synthesis of versatile hydrophilic magnetite nanoparticles. *Ultrason. Sonochem.* **2012**, *19*, 877-882, <https://doi.org/10.1016/j.ultsonch.2011.12.007>.
15. Manikandan, A.; Vijaya, J.J.; Mary, J.A.; Kennedy, L.J.; Dinesh, A. Structural, optical and magnetic properties of Fe₃O₄ nanoparticles prepared by a facile microwave combustion method. *Journal of Industrial and Engineering Chemistry* **2014**, *20*, 2077-2085, <https://doi.org/10.1016/j.jiec.2013.09.035>.
16. Rajiv, P.; Bavadarani, B.; Kumar, M.N.; Vanathi, P. Synthesis and characterization of biogenic iron oxide nanoparticles using green chemistry approach and evaluating their biological activities. *Biocatalysis and Agricultural Biotechnology* **2017**, *12*, 45-49, <https://doi.org/10.1016/j.bcab.2017.08.015>.
17. Mittal, A.K.; Chisti, Y.; Banerjee, U.C. Synthesis of metallic nanoparticles using plant extracts. *Biotechnol. Adv.* **2013**, *31*, 346-356, <https://doi.org/10.1016/j.biotechadv.2013.01.003>.

18. Raveendran, P.; Fu, J.; Wallen, S.L. Completely “Green” Synthesis and Stabilization of Metal Nanoparticles. *J. Am. Chem. Soc.* **2003**, *125*, 13940-13941, <https://doi.org/10.1021/ja029267j>.
19. Azizi, A. Green Synthesis of Fe₃O₄ Nanoparticles and Its Application in Preparation of Fe₃O₄/Cellulose Magnetic Nanocomposite: A Suitable Proposal for Drug Delivery Systems. *Journal of Inorganic and Organometallic Polymers and Materials* **2020**, *30*, 3552-3561, <https://doi.org/10.1007/s10904-020-01500-1>.
20. Mahdavi, M.; Namvar, F.; Ahmad, M.B.; Mohamad, R. Green biosynthesis and characterization of magnetic iron oxide (Fe₃O₄) nanoparticles using seaweed (*Sargassum muticum*) aqueous extract. *Molecules* **2013**, *18*, 5954-5964, <https://doi.org/10.3390/molecules18055954>.
21. Prasad, K.S.; Gandhi, P.; Selvaraj, K. Synthesis of green nano iron particles (GnIP) and their application in adsorptive removal of As(III) and As(V) from aqueous solution. *Appl. Surf. Sci.* **2014**, *317*, 1052-1059, <https://doi.org/10.1016/j.apsusc.2014.09.042>.
22. Abosi, A.O.; Raseroka, B.H. In vivo antimalarial activity of *Vernonia amygdalina*. *Br. J. Biomed. Sci.* **2003**, *60*, 89-91, <https://doi.org/10.1080/09674845.2003.11783680>.
23. Farombi, E.O.; Owoeye, O. Antioxidative and chemopreventive properties of *Vernonia amygdalina* and *Garcinia* biflavonoid. *Int. J. Environ. Res. Public Health* **2011**, *8*, 2533-2555, <https://doi.org/10.3390/ijerph8062533>.
24. Erasto, P.; Grierson, D.S.; Afolayan, A.J. Antioxidant Constituents in *Vernonia amygdalina*. Leaves. *Pharm. Biol.* **2007**, *45*, 195-199, <https://doi.org/10.1080/13880200701213070>.
25. Mekoya, A.; Oosting, S.J.; Fernandez-Rivera, S.; Van der Zijpp, A.J. Multipurpose fodder trees in the Ethiopian highlands: Farmers’ preference and relationship of indigenous knowledge of feed value with laboratory indicators. *Agricultural Systems* **2008**, *96*, 184-194, <https://doi.org/10.1016/j.agsy.2007.08.001>.
26. Habtemariam, A.B.; Oumer, M. Plant Extract Mediated Synthesis of Nickel Oxide Nanoparticles. *Mat Int* **2020**, *2*, 205-209, <https://doi.org/10.33263/Materials22.205209>.
27. Baudot, C.; Tan, C.M.; Kong, J.C. FTIR spectroscopy as a tool for nano-material characterization. *Infrared Physics & Technology* **2010**, *53*, 434-438, <https://doi.org/10.1016/j.infrared.2010.09.002>.
28. Vasantharaj, S.; Sathiyavimal, S.; Senthilkumar, P.; LewisOscar, F.; Pugazhendhi, A. Biosynthesis of iron oxide nanoparticles using leaf extract of *Ruellia tuberosa*: Antimicrobial properties and their applications in photocatalytic degradation. *J. Photochem. Photobiol. B: Biol.* **2019**, *192*, 74-82, <https://doi.org/10.1016/j.jphotobiol.2018.12.025>.